Evidence of Defect-Promoted Reactivity for Epoxidation of Propylene in Titanosilicate (TS-1) Catalysts: A DFT Study

David H. Wells, Jr.,[‡] W. Nicholas Delgass,[†] and Kendall T. Thomson*

Contribution from the School of Chemical Engineering, Purdue University, West Lafayette, Indiana 47907

Received August 4, 2003; E-mail: thomsonk@ecn.purdue.edu

Abstract: Our density functional theory study of hydroperoxy (OOH) intermediates on various model titanosilicalite (TS-1) Ti centers explores how microstructural aspects of Ti sites effect propylene epoxidation reactivity and shows that Ti sites located adjacent to Si vacancies in the TS-1 lattice are more reactive than fully coordinated Ti sites, which we find do not react at all. We show that propylene epoxidation near a Si-vacancy occurs through a sequential pathway where H_2O_2 first forms a hydroperoxy intermediate Ti−OOH (15.4 kcal/mol activation energy) and then reacts with propylene by proximal oxygen abstraction (9.3 kcal/mol activation energy). The abstraction step is greatly facilitated through a simultaneous hydride transfer involving neighboring terminal silanol groups arising from the Si vacancy. The transition state for this step exhibits 6-fold oxygen coordination on Ti, and we conclude that the less constrained environment of Ti adjacent to a vacancy accounts for greater transition state stability by allowing relaxation to a more octahedral geometry. These results also show that the reactive hydroperoxy intermediates are generally characterized by smaller electron populations on the proximal oxygen atom compared to nonreactive intermediates and greater O−O polarization−providing a potential means of computationally screening novel titanosilicate structures for epoxidation reactivity.

Introduction

With the advent of sophisticated computational chemistry techniques, researchers are more and more getting into the business of *computational catalyst design*—the act of using computer simulations and software tools to both analyze and design better catalysts. Thanks to the ever growing power of microprocessors and to the incorporation of modern electronic density functional theory (DFT) methods, *computational catalysis* is today on par with classical experimental analyses. Combined theoretical and experimental strategies are now at the point where theory and experiment can drive each other to a better understanding of catalyst function. The timing of these synergistic efforts could not be better. With the continuous discovery of new micro- and nanoporous materials seen of late,[3,4] researchers have at their disposal a diverse selection of possible frameworks to test for breakthrough catalyst formulations.

To show the power of computational catalysis along these lines, we applied this approach to a longstanding, important problem in the catalysis field. For decades, chemists have been frustrated in their attempts to formulate direct epoxidation pathways from olefins by the preference for allylic hydrogen to undergo abstraction—leading to nonepoxide oxygenates. This fact is perhaps best observed on silver-based epoxidation catalysts, on which direct oxidation of propylene to CO_2 is 30 times faster than for ethylene (which contains no allylic hydrogens).[5] The recent discovery of Haruta,[6] and subsequent work by other investigators,[7,8] showing that nanoscale Au clusters deposited on tetrahedral titanium in oxide supports are active for direct gas-phase epoxidation using H_2 and O_2 has opened the door to direct epoxidation routes that might be commercially viable. To date, however, sufficiently active catalysts for the epoxidation of propylene (the simplest allylic olefin) using H_2 and O_2 remain elusive despite the interest in a gas-phase green chemistry for the production of propylene oxide.

To address this problem, it is appropriate to consider the connection between Au/TS-1catalyst microstructure and epoxidation reactivity. This is in fact the goal of computational catalyst design, to relate changes in atomic configurations of the catalyst to activity using computational chemistry. We address Au functionality of this catalyst in other work,[9] but briefly, the thesis is that hydrogen peroxide forms from H_2 and O_2 reacting on small atomic-sized Au clusters. Subsequent epoxidation by hydrogen peroxide over TS-1 is the step we subject to investigation here. In this paper we demonstrate that

[†] E-mail: delgass@ecn.purdue.edu.
[‡] E-mail: wellsd@purdue.edu.

(1) Clerici, M. G.; Bellussi, G.; Romano, U. *J. Catal.* **1991**, *129*, 159−167.
(2) Munakata, H.; Oumi, Y.; Miyamoto, A. *J. Phys. Chem. B* **2001**, *105*, 3493−3501.
(3) Rolison, D. R. *Science* **2003**, *299*, 1698.
(4) Davis, M. E. *Nature* **2002**, *417*, 813.
(5) Shetti, V. N.; Manikandan, P.; Srinivas, D.; Ratnasamy, P. *J. Catal.* **2003**, *216*, 461−467.
(6) Uphade, B. S.; Akita, T.; Nakamura, T.; Haruta, M. *Am. Chem. Soc., Div. Pet. Chem.* **1996**, *41*, 71.
(7) Stangland, E. E.; Stavens, K. B.; Andres, R. P.; Delgass, W. N. *J. Catal.* **2000**, *191*, 332−347.
(8) Nijhuis, T. A.; Huizinga, B. J.; Makkee, M.; Moulijn, J. A. *Ind. Eng. Chem. Res.* **1999**, *38*, 884−891.
(9) Wells, D. H.; Delgass, W. N.; Thomson, K. T. *J. Catal.* **2004**, *submitted*.
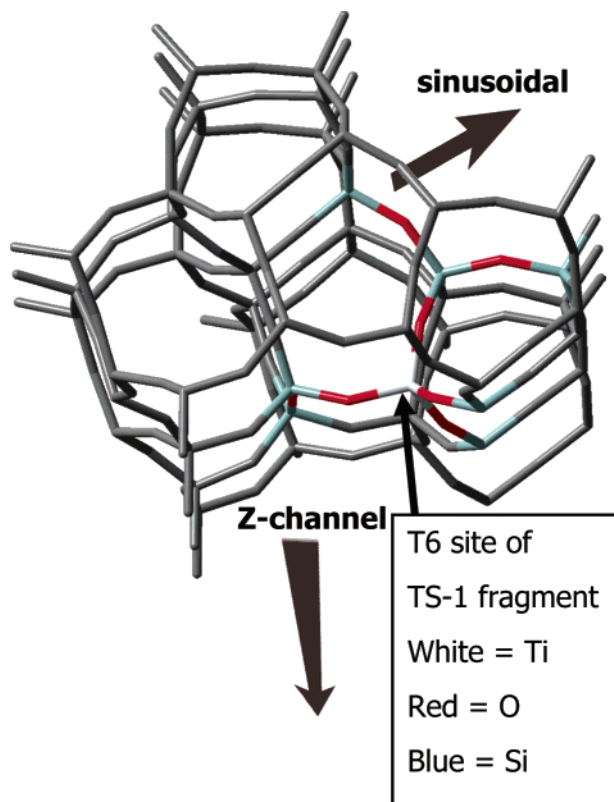
Figure 1. Portion of the crystal structure of microporous titanium silicalite (TS-1) zeolite.[1]

Figure 2. Schematic view of a fully tetrahedrally bonded Ti ion substituted for a Si ion at one of the lattice positions of TS-1 (A) and the same Ti site located near a silicon vacancy terminated with hydrogen atoms forming a silanol nest (B).

the microstructural aspect of the Ti active site is crucial for epoxidation reactivity and furthermore that *Ti sites located near Si vacancies in Ti-substituted silicate lattices provide a significant advantage for epoxidation.* We believe this result could be far-reaching as it may be applicable to a broader class of reactions in tectosilicate catalyst supports in general. In addition, changes on the proximal oxygen and associated O—O polarization in the hydroperoxy intermediate has emerged as a potential descriptor of propensity for epoxidation activity.

Experimental Section

Propylene Epoxidation. Even in light of the success of H_2O_2 liquid-phase epoxidation systems using microporous titanium silicalite (TS-1) zeolite catalysts[1] (see Figure 1), efforts to develop Au-supported TS-1 catalysts for H_2/O_2 epoxidation have resulted in only modest success to date.[7,8,10] Au/TS-1 catalysts for propylene epoxidation by H_2 and O_2 are limited by low conversion—despite exhibiting relatively high propylene oxide selectivity (>90%). While catalysts recently prepared in our lab (with loadings of Au <0.2 wt % and Ti <2.5%) show greatly improved stability, they still only achieve a maximum propylene conversion of 6.5%.[11] Further improvements in these catalysts will come from a better understanding of the chemistry involved. Because low Au and Ti levels in good catalysts make spectroscopic investigation a challenge, our computational approach allows detailed and targeted analysis of both the Ti site and the Au promotion of such sites.[12]

Catalytic activity[1] in TS-1 is known to occur at Ti sites internal to the crystallite, which are, ideally, fully tetrahedrally bonded in the TS-1 lattice as shown schematically in Figure 2A. Prior computational work
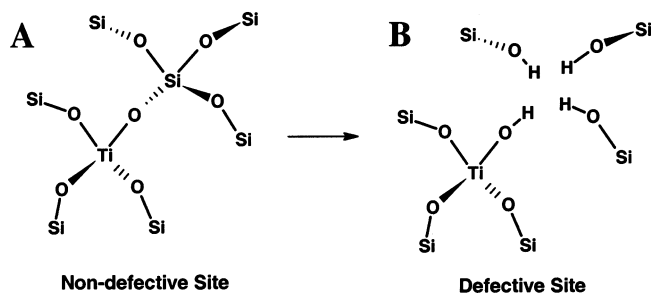
with density functional theory (DFT) on the active site of TS-1 epoxidation catalysts[2,13−21] has focused on studying the nature of Ti/H_2O_2 activity and has led to significant progress in our understanding of epoxidation catalysis. However, these studies utilized cluster approximations to the TS-1 lattice that concentrate on surface Ti site models with very small cluster representations, which we believe may be inadequate to represent the Ti site in the TS-1 lattice. Further, previous cluster models that directly address internal Ti-site geometries may not be large enough to adequately detect important steric limitations of the fully coordinated internal Ti sites. In this paper we describe DFT calculations conducted on representations of TS-1 which more accurately capture the geometry and chemistry of active internal Ti substitution sites. In addition to the Ti ion, we include from six to seven of the neighboring silicon ion positions. Prior studies have utilized at most four neighboring silicon ions in the cluster model.[2,13−21]

A critical component of our Ti site model is the recognition that aside from a fully coordinated (nondefect) Ti site, Ti may also reside near a Si vacancy (defect) in the TS-1 lattice (see Figure 2). Tetrahedral sites with Si vacancies adjacent to titanium substitutions may occur randomly or even more frequently if the lattice strain of a Ti substitution is partly relieved by a neighboring defect. This possibility is highlighted by the findings of Lamberti et al.[22] who identified sites of high Ti substitution (T6, T7, T11, and possibly T10). These same sites were also described as preferred sites for vacancies in defective silicalite. Within this particular subset of the 12 tetrahedral sites there are combinations of neighbors which would allow a Ti substitution to neighbor a defect. For example, the T7 site is neighbored by T7 and T11. The T11 site is neighbored by T7 and T10. The T10 site is neighbored by T10 and T11. The T6 site has neighbors T2, T3, T5, and T9. The defect cluster studied here assumes the defect at the T5 neighbor site. In this paper we examine a simple approximation to the combination of Ti at T6 with a defect at T5 using only one of the three neighboring silanol groups that heal the T5 defect. Future work will examine this system with all neighboring silanol groups of the defect and consider other combinations of Ti and the defect sites. Based on preliminary work of this nature, we feel the relevant effects are captured in this simplified model. Random placement of Ti and vacancies on these sites lead to many combinations with Ti neighboring a defect. Because TS-1 is so highly connected, even randomly sited defects and Ti substitutions at low concentrations lead to a relatively high occurrence of defect/Ti neighbor pairs. In simulations of this

(10) Qi, C.; Akita, T.; Okumura, M.; Haruta, M. *Appl. Catal. A: Gen.* **2001**, *218*, 81−89.
(11) Yap, N.; Delgass, W. N. *J. Catal.*, submitted for publication.
(12) Wells, D. H.; Delgass, W. N.; Thomson, K. T. *J. Am. Chem. Soc.*, submitted for publication.
(13) Wu, Y.-D.; Lai, D. K. W. *J. Org. Chem.* **1995**, *60*, 673−680.
(14) Karlsen, E.; Schöffel, K. *Catalysis Today* **1996**, *32*, 107−114.
(15) Neurock, M.; Manzer, L. E. *Chem. Commun.* **1996**, 1133−1134.
(16) Sinclair, P. E.; Sankar, G.; Catlow, C. R. A.; Thomas, J. M.; Maschmeyer, T. *J. Phys. Chem. B* **1997**, *101*, 4232−4237.
(17) Sinclair, P. E.; Catlow, C. R. A. *J. Phys. Chem. B* **1999**, *103*, 1084−1095.
(18) Tantanak, D.; Vincent, M. A.; Hillier, I. H. *Chem. Commun.* **1998**, 1031−1032.
(19) Vayssilov, G. N.; van Santen, R. A. *J. Catal.* **1998**, *175*, 170−174.
(20) Sever, R. R.; Root, T. W. *J. Phys. Chem. B* **2003**, *107*, 4080−4089.
(21) Sever, R. R.; Root, T. W. *J. Phys. Chem. B* **2003**, *107*, 4090−4099.
(22) Henry, P. F.; Weller, M. T.; Wilson, C. C. *J. Phys. Chem. B* **2001**, *105*, 7452−7458.
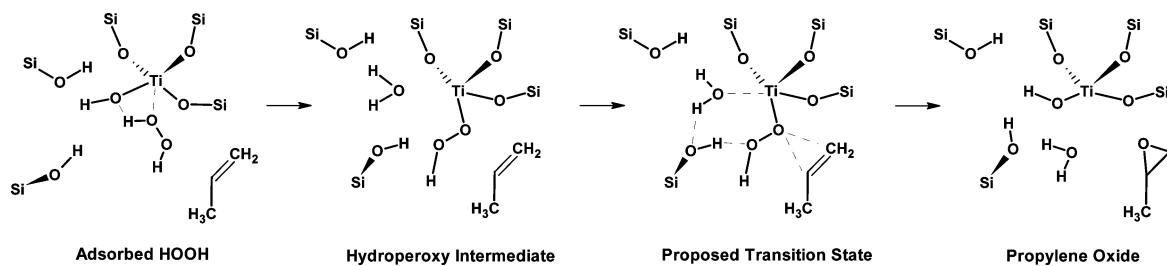
Figure 3. Mechanism for HOOH/propylene epoxidation to PO on a defective Ti site in TS-1.

structure we found approximately 0.8 Ti/defect pairs per unit cell using a 2% Ti substitution level, 8% defect frequency, and random location of substitution and defect occurrences on the Lamberti subset (T6, T7, T11, and T10). This surprisingly high frequency of occurrence justifies consideration of both types of T-site models, defect and nondefect, as we fully expect the differing structural environments of each to result in different activity.

In what follows, we present DFT-based calculations of production from propylene on H_2O_2 activated Ti sites using both a "nondefect" and "defect" representation of the site geometry. The purpose is to compare epoxidation reactivity between these alternative geometries by predicting reaction pathways for epoxidation and quantifying the corresponding potential energy landscapes. The rest of this article is organized as follows, first the computational techniques are described including the nature of the cluster models used in our calculations, next the reactivity of the nondefect and defect Ti site models are discussed, and we summarize with conclusions.

Computational Method. All calculations were conducted using the Gaussian98[23] suite of programs. We used density functional theory (DFT) with the exchange functional[24] of Becke's 1988 and Purdue-Wang's 1991 correlation energy functional (BPW91).[25–28] The Los Alamos LANL2DZ[29] effective core pseudopotentials (ECP) and valence double-ζ basis set for silicon and titanium were utilized as well as the D95[30] full double-ζ basis sets for carbon, hydrogen, and oxygen. The choice of functional was dictated in part by other research being conducted in conjunction with this work, which involves small Au clusters. Since the metallic clusters are poorly represented by B3LYP,[23] we have chosen BPW91 as a reasonably equivalent alternative. Basis set superposition errors were not calculated as they would be a small factor of several kcal/mol and a relatively constant energetic offset across the cluster models we compared. All energies and energy differences are calculated for 0 K without zero point energy (ZPE) corrections. The ZPE corrections would likely be similar for each of these clusters and thus would not influence conclusions based on the relative energies.

(23) Frisch, M. J.; Trucks, G. W.; Schlegel, H. B.; Scuseria, G. E.; Robb, M. A.; Cheeseman, J. R.; Zakrzewski, V. G.; Jr., J. A. M.; Stratmann, R. E.; Burant, J. C.; Dapprich, S.; Millam, J. M.; Daniels, A. D.; Kudin, K. N.; Strain, M. C.; Farkas, O.; Tomasi, J.; Barone, V.; Cossi, M.; Cammi, R.; Mennucci, B.; Pomelli, C.; Adamo, C.; Clifford, S.; Ochterski, J.; Petersson, G. A.; Ayala, P. Y.; Cui, Q.; Morokuma, K.; Malick, D. K.; Rabuck, A. D.; Raghavachari, K.; Foresman, J. B.; Cioslowski, J.; Ortiz, J. V.; Baboul, A. G.; Stefanov, B. B.; Liu, G.; Liashenko, A.; Piskorz, P.; Komaromi, I.; Gomperts, R.; Martin, R. L.; Fox, D. J.; Keith, T.; Al-Laham, M. A.; Peng, C. Y.; Nanayakkara, A.; Challacombe, M.; Gill, P. M. W.; Johnson, B.; Chen, W.; Wong, M. W.; Andres, J. L.; Gonzalez, C.; Head-Gordon, M.; Replogle, E. S.; Pople, J. A.; Revision A.8 ed.; Gaussian Inc.: Pittsburgh, PA, 1998.
(24) Becke, A. D. *Phys. Rev. A* **1988**, *38*, 3098.
(25) Burke, K.; Perdew, J. P.; Wang, Y. In *Electronic Density Functional Theory: Recent Progress and New Directions*; Das, M. P., Ed.; Plenum: 1998.
(26) Perdew, J. P. In *Electronic Structure of Solids '91*; Eschrig, H., Ed.; Akademie Verlag: Berlin, 1991; p 11.
(27) Perdew, J. P.; Chevary, J. A.; Vosko, S. H.; Jackson, K. A.; Pederson, M. R.; Singh, D. J.; Fiolhais, C. *Phys. Rev. B* **1992**, *46*.
(28) Perdew, J. P.; Chevary, J. A.; Vosko, S. H.; Jackson, K. A.; Pederson, M. R.; Singh, D. J.; Fiolhais, C. *Phys. Rev. B* **1993**, *48*.
(29) Hay, P. J.; Wadt, W. R. *J. Chem. Phys.* **1985**, *82*, 270.
(30) Dunning, J., T. H.; Hay, P. J. In *Modern Theoretical Chemistry*; H. F. Schaefer, I., Eds.; Plenum: New York, 1976; Vol. 3, p 1.

We used terminated cluster representations to model the Ti-sites in TS-1 for both the defect and nondefect cases, and the T6 crystallographic position of the TS-1 crystal structure as the Ti substitution site. Though questions remain about which of the 12 different tetrahedral sites in the orthorhombic structure of TS-1 host Ti substitutions, the finding by Lamberti et al. that 5–8% of the T sites in well-made TS-1 are defective, based on neutron diffraction work, is important.[31] When a Ti-substituted metal site neighbors a Si vacancy, the resulting structure is substantially different from nondefect Ti sites, as is evident in Figure 2b. Similarly, internal defect Ti sites are also different from Ti-substituted metal sites at the outer crystal surface, where the geometric constraints are lower and neighbor geometry is arbitrary. Surface Ti sites have no nearby silanol groups to coordinate with reactant ligands centered on the Ti site. Hence, any choice of crystallographic metal position inside the crystal will adequately discern variations in activity for which we are interested, namely, defect versus nondefect Ti sites.

Our T6 cluster model approximation uses lattice positions from Koningsveld for ZSM-5.[32] The selected cluster includes all nearest neighbor silicon ions and a few selected second nearest neighbor silicon ions (total number of eight metal atoms). Both clusters are terminated by substituting H ions at O ion lattice positions, adjusting their bond lengths to optimized Si–H lengths for our DFT approximation (BPW91/ LANL2DZ) and fixing hydrogen positions to crystallographic data during structural minimization. No oxygen, silicon, or titanium ion locations were fixed during any of these calculations, thus silicon ions anchored by fixed hydrogen ion positions can be considered "tethered". None of the atoms in propylene was constrained in any way.

Based in part on published computational work,[2,13–21] we hypothesize the following epoxidation route at the Ti defect site (see Figure 3): (1) H_2O_2 insertion at the Ti center accompanied by hydrolysis of the terminal Ti hydroxyl group to form an active hydroperoxy intermediate, (2) propylene physisorption near the Ti/hydroperoxy intermediate site, (3) proximal oxygen abstraction to form propylene oxide, and (4) desorption of water and PO. In the case of the nondefect Ti site, the corresponding bridging oxygen would be protonated in place of hydrolysis in step (1). This proposed pathway was used to postulate initial geometries for reactant and product states as well as for reactive intermediates.

The approach we used in each case (defect and nondefect models) was to first identify the stable intermediate geometries. Full structural relaxation subject to the cluster constraints described above was performed for these computations. Where appropriate, transition-state geometries were found using the STQN method of Schlegel and co-workers as implemented in Gaussian98.[23] Reactions with propylene near active Ti/hydroperoxy sites were simulated by positioning propylene near the stable relaxed geometry of each Ti/hydroperoxy intermediate and letting the complex relax. The initial position of propylene was based on an analysis of frontier orbitals, which were used to establish the preferred overlap orientation between the LUMO of the oxygen moiety and the HOMO of propylene (the double bond π electrons).

(31) Lamberti, C.; Bordiga, S.; Zecchina, A.; Artioli, G.; Marra, G. L.; Spanò, G. *J. Am. Chem. Soc.* **2001**, *123*, 2204–2212.
(32) Koningsveld, H. v.; Bekkum, H. v.; Jansen, J. C. *Acta Crystallogr.* **1987**, *B43*, 127–132.
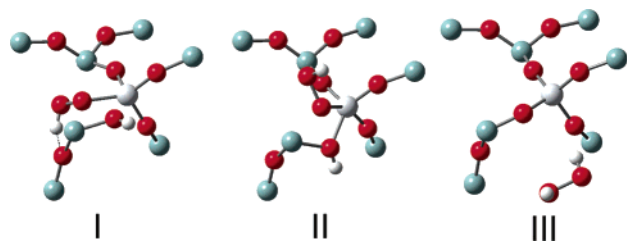
Figure 4. T6 cluster model (Ti = large white, O = red, Si = blue, H = small white spheres). (I) H_2O_2 addition to the oxygen atom coordinated to the Ti center has led to a hydroperoxy species hydrogen bonded to lattice oxygen. (II) H_2O_2 addition to the oxygen atom coordinated to the Ti center leading to a hydroperoxy species protruding into a sinusoidal channel of TS-1. (III) H_2O_2 is physisorbed on the Ti center with no hydroperoxy species formed.

Results

Nondefect Model. For the nondefect model, two different stable hydroperoxy intermediates were found by structural relaxation (geometries **I** and **II** in Figure 4), representing hydroperoxy fragments attached to Ti in different orientations. The formation of a hydroperoxy intermediate results in the concurrent formation of a neighbor hydroxyl group Si—OH, which, due to proximity, affects the final geometry of the intermediate. The optimized structure **I** is slightly higher in energy (by 0.6 kcal/mol) than geometry **II** and the formation of both geometries from H_2O_2 was found to be endothermic (+6.5 and +5.9 kcal/mol for **I** and **II**). Figure 4 illustrates how the —OOH group(I) is located back into the crystal structure to the point that the terminal H ion is hydrogen bonded to a more distant lattice oxygen. The OOH group of geometry **II** (see Figure 4) is much more accessible, as it protrudes into both the sinusoidal and z-channel pores of the zeolite.

In both these cases, however, as propylene was brought in the vicinity, the interaction between propylene and the hydroperoxy group was found to be highly repulsive, and we could not find a viable pathway that led to a reaction. The Mulliken electron populations on the proximal oxygen ions were approximately −0.5, which we will show was the least electrophilic (most negative) of all the intermediates considered here. For comparison, the TS-1 lattice oxygens all had Mulliken populations of −0.8 or lower (more negative).

Previous calculations suggest that H_2O_2 can also physisorb on the Ti site of TS-1.[19] We attempted to repeat this calculation, and using our nondefect cluster, we calculated an adsorption energy of −5.4 kcal/mol (exothermic). This physisorbed configuration (geometry **III** in Figure 4) was found to be 11.3 kcal/mol lower in energy compared to geometry **II**. We observed that the Mulliken population on the active oxygen in **III** is −0.405, similar to the unreactive (nondefect site) complexes (vide infra). The closest O—Ti distance between an oxygen in H_2O_2 and the Ti site in the constrained cluster model of Vayssilov and van Santen was 2.91 Å.[19] In contrast, we found this O—Ti distance to be 3.78 Å in **III** and conclude that steric repulsions from the neighboring lattice oxygens contribute significantly to the low physisorbed energy of **III**. Vayssilov and van Santen report that physisorbed H_2O_2 reacts with ethylene to form ethylene oxide; however, based on our analysis with a more realistic cluster representation, we feel this is unlikely for propylene.

Defect Model. We would expect the situation were Ti resides in a defect geometry (adjacent to a Si-vacancy) to be much more
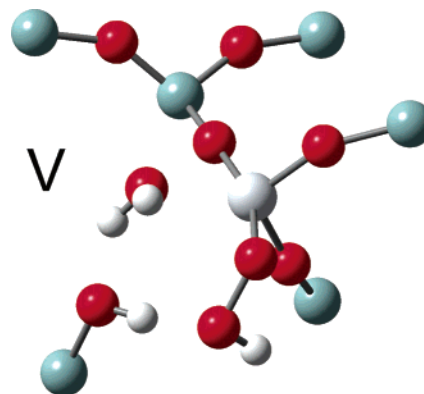

Figure 5. T6 cluster model with defect site (Ti = large white, O = red, Si = blue, H = small white spheres) including a coordinated H_2O molecule. H atoms are fixed rigidly in space and simulate the constraints imposed by the full lattice.

favorable for reaction simply due to the issue of accessibility of the reagents to the Ti site and the additional available space for transition-state stabilization. More specifically, the absence of one Si atom should reduce steric repulsions and provide greater flexibility of the Ti site to accommodate lower energy configurations of reactive intermediates as well as transition states.

Our calculations show that the addition of H_2O_2 to the hydroxyl group on Ti leads to the hydroperoxy intermediate geometry **V** shown in Figure 5. The energetics of the entire reaction pathway are shown in Figure 7. As seen, the formation of **V** was found to be exothermic (−9 kcal/mol) compared to endothermic for the nondefect site. The hydroperoxy group has η-1 coordination, which is stabilized by hydrogen bonding to an oxygen in the adjacent silanol nest—in contrast to the η-2 coordination observed in simplified models of the Ti site found in the literature.[14] Further, the Mulliken population for the proximal oxygen in this intermediate was −0.357, much more electrophilic than the hydroperoxy oxygens in **I** and **II**.

Unlike for the nondefect model, bringing propylene into proximity with the intermediate geometry **V** leads to a viable reaction pathway to propylene oxide. The activation barrier for this reaction was found to be 9.3 kcal/mol, and the energy of reaction was highly exothermic (−41.1 kcal/mol). The transition state for this reaction (geometry **V**‡) is shown in Figure 6 and the entire reaction pathway for the defect site is schematically represented in Figure 3.

The O-abstraction step was observed to proceed through a dual hydride transfer mechanism involving adsorbed H_2O (generated from the hydroperoxy intermediate formation step) and a neighboring terminated Si—OH group (see Figure 3). In this process, the nonabstracted oxygen atom of the OOH intermediate hydrogen bonds with a terminal hydrogen on a neighboring silanol group, ultimately forming a new water molecule. The resulting bare oxygen reforms a silanol group by abstracting hydrogen from the initial water molecule, which recoordinates as an OH group with Ti, completing the catalytic cycle. The product state of this reaction consists of adsorbed propylene oxide, a newly generated H_2O molecule (formally the hydroperoxy group), and the original terminated Si—OH. The dual hydride transfer appears to occur simultaneously and is not possible for the nondefect model. Also, this phenomenon
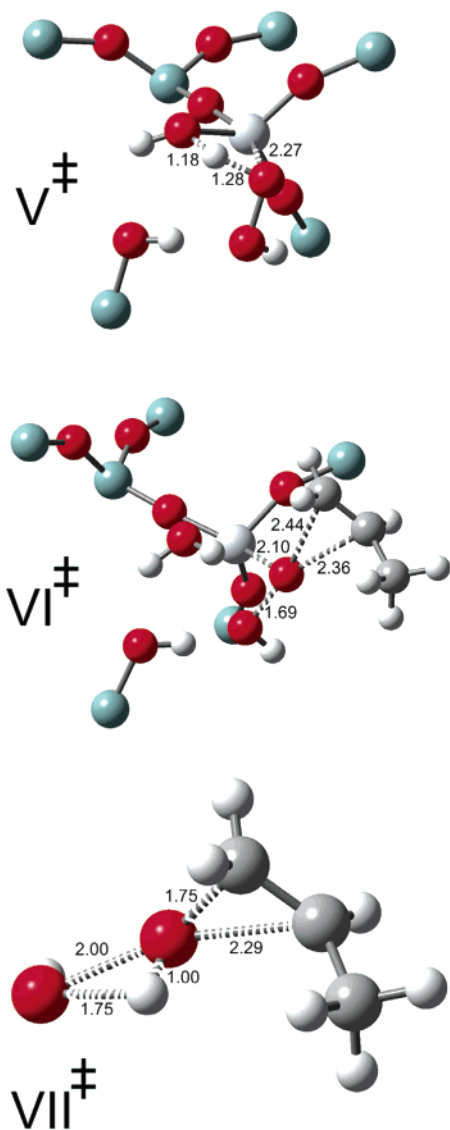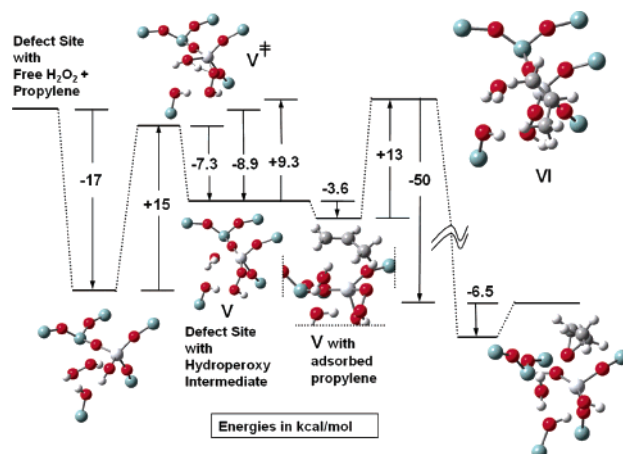
Figure 7. T6 cluster model with defect site (Ti = large white, O = red, Si = blue, H = small white spheres) including a coordinated H_2O molecule. Note the terminating H atoms on Si at the periphery of the cluster are removed for clarity. In the calculations these H atoms are fixed rigidly in space and simulate the constraints imposed by the full lattice. All energies are in kcal/mol.
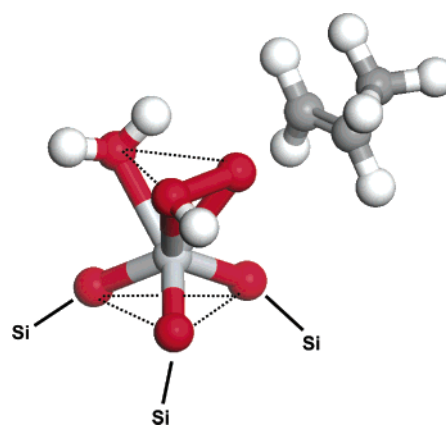

Figure 8. Close-up of the defect Ti site transition state for proximal oxygen abstraction. Oxygen atoms are in red, hydrogen atoms in white, and carbon atoms in gray. Ti is at the center of the 6-fold coordination polyhedron.

Figure 6. T6 cluster model (Ti = large white, O = red, Si = blue, H = small white spheres) of the transition state for propylene epoxidate formation from a hydroperoxy intermediate over the defect site. Bond lengths of those bonds breaking or forming during the transition state are shown in angstroms (the terminating H atoms on Si at the periphery of the cluster are removed for clarity). (V) Transition state for hydroperoxy intermediate formation from H_2O, (VI) Transition State for reaction of hydroperoxy intermediate on defect T6 site with propylene. (VII) Gas-phase transition state for propylene + H_2O_2 → hydrogen peroxide.

would not be observed in small cluster models that neglect neighboring Si–OH contributions.

Discussion

Based on our calculations, we note that for the case of internal (nonsurface) Ti sites in TS-1, Ti located adjacent to Si vacancies provides a highly reactive pathway to epoxidation compared to Ti associated with nondefects. Indeed, we failed to even find a pathway for epoxidation in the nondefect model even presuming stable hydroperoxy intermediates exist.

We believe there are a number of reasons why this is so. First, to understand why tetrahedral Ti is active for epoxidation (and why purely siliceous frameworks do not exhibit activity) we studied the transition state for epoxidation (geometry $V^{\ddagger}$ in Figure 7) in more detail. Figure 8 shows the transition state

structure in a more focused light, concentrating on the geometry of the Ti coordination. We find that the active Ti during the TS is 6-fold coordinated, forming a distorted octahedral complex involving two Si–O–Ti bridges, an adsorbed water oxygen, and both oxygens from the hydroperoxy complex. Ti is well-known to exist in titanosilicate structures with octahedral coordination, which explains why the transition state is relatively stable, compared to Si. The reason for this stability is likely the existence of the unfilled d-band of Ti and the physical nature of s–d hybridization—which differs from sp^3 hybridization found in Si bonding.

We expect that the more octahedral the transition state is in a given framework, the more stable the transition state. The effect of the Ti defect site is 2-fold in this regard. First, the site is more open in structure, allowing adsorbed water to coordinate nearby after hydroperoxy formation. Second, the defect Ti site is more flexible, providing the potential for greater stabilization through structural relaxation during the transition-state formation. In particular, the adsorbed water molecule that serves as one of the 6-fold coordinating oxygens is much more labile compared to a Si–O–Ti link that would replace it in the corresponding nondefect analogue. Hence, we believe the

Table 1. Comparison of OOH Bond Parameters in Intermediates and Reactants[a]

reactant/intermediate	O–O bond length, Å	O–O polarization proximal–distal[g]	proximal O Mulliken pop	reactive[f]
nondefect sites				
T6(H)−O−OH (down)	1.490	−0.147	−0.50	N
T6(H)−O−OH (up)	1.507	−0.190	−0.50	N
chemisorbed on closed site				
T6(HO−OH)ads	1.529[e]	−0.021[e]	−0.41	Y (van Santen)
gas-phase H_2O_2	1.536	0.0	−0.38	N[d]
defect site[b]				
T6(H)−O−OH	1.532	0.059	−0.36	Y[c]
Munakata O−O				
T6−O−O−Si	1.583	0.208	−0.33	Y[c]

[a] BPW91/LANL2DZ density functional theory approximation. [b] Includes H_2O molecule coordinated to Ti site (remnant from H_2O_2). [c] Proximal oxygen to Ti is the reactive oxygen [d] Activation barrier is 17 kcal/mol [e] Values from cluster calculations in this work [f] Proximity of propylene to the reactive oxygen leads to an energetically downhill path to propylene oxide (Y) or is repulsive and/or requires an activation energy to react (N). [g] Mulliken electron population of proximal oxygen−Mulliken electron population of distal oxygen.
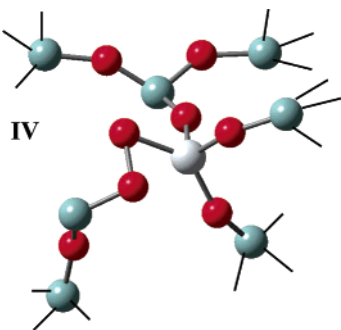

Figure 9. T6 cluster model (Ti = large white, O = red, Si = blue, H = small white spheres) of the intermediate proposed by Munakata et al.[2] Note the terminating H atoms on Si at the periphery of the cluster are removed for clarity. In the calculations these H atoms are fixed rigidly in space and simulate the constraints imposed by the full lattice.

nondefective site is not active due to the fact that the transition state is too rigid and cannot relax enough to stabilize itself.

The transition state for epoxidation (geometry **VI‡**) can be compared to the un-catalyzed transition state for epoxidation computed in a vacuum (geometry **VII‡** in Figure 6). In both cases oxygen is transferred to the propylene double bond. However, the activation energy for gas-phase epoxidation (see geometry **VII‡** in Figure 6) is 17 kcal/mol compared with the 9.3 kcal/mol on the defect site model. The gas-phase activation energy is higher despite a closer approach of the transferring oxygen to a double bond carbon. The overriding factor is apparently the greater stretch of the oxygen−oxygen bond in the gas-phase reaction. At the transition state in the gas phase (**VII‡**, Figure 6), the oxygen−oxygen bond is 2.00 Å vs 1.69 Å in the catalyzed transition state **VI‡**. The oxygens in the hydroperoxy group, which are in a η-1 configuration in the reactive intermediate, shift to a η-2 position in the epoxidation transition state.

An additional intermediate configuration (shown in Figure 9) was proposed recently by Munakata et al.[2] in which hydrogen peroxide reacts with an unhydrolyzed Ti−O−Si bond to yield H_2O and Ti−O−O−Si. We find the energy of formation for the unhydrated intermediate (geometry **IV**) to be +20 kcal/mol on the nondefect site. We conclude that, though highly active once formed, the activation energy barrier to the formation of the hydrated intermediate reported by Munakata et al. as 16.5 kcal/mol is slightly higher than the formation barrier to other reactive intermediates (vide supra). However, further work is needed to explore this possibility.

Examining the Mulliken populations of the hydroperoxy intermediates that result in epoxidation reactivity, we see the interesting result that the active oxygen exhibits populations of approximately −0.4 or greater (less negative). This correlates with the ability of the residual hydroxyl group to readily form a stable bond after epoxidation. In contrast, the hydroperoxy intermediates involved in the nonreactive, nondefect site model had electron populations of −0.5. The Ti−O−O−Si intermediate of Munakata, which we expect to be reactive, had a proximal oxygen charge of −0.33. Since electrophilic attack of the C=C double bond is the presumed mechanism for oxygen abstraction, it is not surprising that electron deficient oxygens are more susceptible to epoxidation.

On the other hand, since the epoxidation route involves simultaneous oxygen abstraction and O−O cleavage at the hydroperoxy intermediate, a more pertinent predictor of reactivity might be the hydroperoxy O−O polarization−defined as the difference in charge between the proximal versus distal oxygens. Table 1 contains a summary of these observations. Clearly we see that reactive hydroperoxy intermediates exhibit a positive polarization value corresponding to greater negative charge concentrated on the distal (nonreactive) oxygen atom. Since this oxygen is involved in protonation to form water after O−O cleavage, it is expected that greater electron concentration would be a factor influencing hydrogen abstraction. These criteria may prove useful as a screening tool for assessing modified catalyst systems for epoxidation as a large number of possible Ti site/defect site combinations exist. We note that such descriptors of reactivity will play an increasingly important role as computational catalysis expands. Reliable descriptors that do not require a full DFT analysis of the reaction pathway will greatly accelerate searches for new catalytic materials.[33]

Conclusions

This work shows that the complexities of TS-1 may hide more complicated epoxidation chemistry than has been earlier realized. Using realistic cluster approximations of a size better suited to adequately describe the extended environments of active Ti sites in TS-1, we have uncovered a new Ti/defect active site which greatly facilitates the epoxidation reaction in DFT computations. The activation barrier to propylene epoxidation with the hydroperoxy intermediate on a Ti/defect site was found to be 9

(33) Norskov, J. K. In *International Symposium on Reaction Kinetics and the Development of Catalytic Processes*; C., W. K., Ed.; Elsevier Science: Amsterdam; Brugge: Belgium, 1999.

kcal/mol. This is lower than the activation energy for epoxidation by either the Munakata intermediate (18 kcal/mol) or the Sinclair and Catlow intermediate (10 kcal/mol), though in these cases ethylene rather than propylene was the olefin examined. Hydroperoxy intermediates formed on internal Ti sites with full tetrahedral coordination to lattice oxygens were found to have a repulsive interaction with propylene. It is beyond the scope of this paper to examine the ethylene reaction on the Ti/defect active site; however, future work addressing this case will allow more direct comparison of activation barriers between the various mechanisms and sites.

We have shown that the epoxidation pathway proceeds in the defect site through a simultaneous hydride transfer mechanism that facilitates the oxygen abstraction by propylene by stabilizing the transition state. It is the ability of Ti to accommodate octahedral coordination—exhibited at the transition state—and the flexibility of the not fully coordinated Ti site near a Si vacancy that drives this stability. In addition, we have identified two potential predictors of reactivity, (1) proximal oxygen charge and (2) O—O polarization, which may be useful in screening novel frameworks for epoxidation activity. Further experimental work is needed to better establish which particular internal Ti site/defect site combinations of TS-1 crystallites are active in gas-phase epoxidation and whether the abundance of particularly active combinations can be controlled to create improved epoxidation catalysts.

JA037741V